Rapid Detection of DNA and RNA Shrimp Viruses Using CRISPR-Based Diagnostics

Samuel R. Major,[a] Matthew J. Harke,[a] Roberto Cruz-Flores,[b*] Arun K. Dhar,[b] Andrea G. Bodnar,[a] Shelly A. Wanamaker[a]

aGloucester Marine Genomics Institute, Gloucester, Massachusetts, USA
bAquaculture Pathology Laboratory, School of Animal and Comparative Biomedical Sciences, The University of Arizona, Tucson, Arizona, USA

ABSTRACT Timely detection of persistent and emerging pathogens is critical to controlling disease spread, particularly in high-density populations with increased contact between individuals and limited-to-no ability to quarantine. Standard molecular diagnostic tests for surveying pathogenic microbes have provided the sensitivity needed for early detection, but lag in time-to-result leading to delayed action. On-site diagnostics alleviate this lag, but current technologies are less sensitive and adaptable than lab-based molecular methods. Towards the development of improved on-site diagnostics, we demonstrated the adaptability of a loop-mediated isothermal amplification-CRISPR coupled technology for detecting DNA and RNA viruses that have greatly impacted shrimp populations worldwide; White Spot Syndrome Virus and Taura Syndrome Virus. Both CRISPR-based fluorescent assays we developed showed similar sensitivity and accuracy for viral detection and load quantification to real-time PCR. Additionally, both assays specifically targeted their respective virus with no false positives detected in animals infected with other common pathogens or in certified specific pathogen-free animals.

IMPORTANCE The Pacific white shrimp (*Penaeus vannamei*) is one of the most valuable aquaculture species in the world but has suffered major economic losses from outbreaks of White Spot Syndrome Virus and Taura Syndrome Virus. Rapid detection of these viruses can improve aquaculture practices by enabling more timely action to be taken to combat disease outbreaks. Highly sensitive, specific, and robust CRISPR-based diagnostic assays such as those developed here have the potential to revolutionize disease management in agriculture and aquaculture helping to promote global food security.

KEYWORDS assay development, diagnostics, pathogens, rapid tests

The ability to rapidly detect disease is a major challenge not just in human health but across all farmed and wild animal health monitoring. While methods for disease detection have advanced the field of molecular diagnostics to the global role it plays today, limitations posed by laboratory-based technologies hinder the ability to quickly respond to disease outbreaks. For example, culturing and molecular diagnostics using PCR-based methods provide the high sensitivity needed for early pathogen detection, but they require laboratory processing (e.g., sophisticated equipment, expensive reagents, and specialized training) leading to long turnaround times for results (several days) and delayed action for disease mitigation (1–4). Contrastingly, immunochromatographic antigen diagnostics are field-deployable, affordable and provide rapid results, but comparatively lack sensitivity and require more time for assay creation resulting in a longer time to respond to emerging pathogens (5). Alternative molecular diagnostics that require less sophisticated equipment like loop-mediated isothermal amplification (LAMP) have recently been developed, but their superior amplification efficiency can stochastically yield false-positive results (6). In human health, CRISPR-based molecular diagnostics, such as the SHERLOCK

(Specific High sensitivity Enzymatic Reporter UnLOCKing) technology, have emerged to overcome the limitations of PCR and antigen tests to enable rapid, sensitive, inexpensive, and accurate on-site detection of viruses and other pathogens (7). SHERLOCK combines the efficiency of isothermal amplification with the specificity of CRISPR detection for highly sensitive, specific, and robust diagnostics that can be used in low resource settings (8). Applications beyond human health in veterinary pathology and disease diagnostics in agriculture and aquaculture settings could have a tremendous impact on domestic and global food security.

The need for rapid, sensitive, and accurate diagnostics in aquaculture is imminent with production expected to double by 2050 to meet the demand of the growing population and being greatly impeded by infectious diseases (9, 10). For example, Pacific white shrimp (*Penaeus vannamei*) production, that accounts for ~25% of all seafood products consumed annually, has suffered major economic losses due to infections caused by viruses like White Spot Syndrome Virus (WSSV) and Taura Syndrome Virus (TSV) (11–13). These diseases have resulted in up to 100% mortality in as few as 7 days (14, 15). The DNA virus WSSV has been the leading cause of economic losses in shrimp aquaculture globally since its emergence in 1991, costing ~$1 billion and reducing global shrimp production by ~10% annually (11). TSV, a single-stranded RNA virus, has caused mass mortality events on at least five continents since its emergence in 1991, with an estimated total loss of $2 billion from 1992 to 1996 (16–18). Although Taura syndrome caused by TSV is no longer causing economic losses to the extent it has in the past, with the current availability and farming of TSV-tolerant shrimp lines (19), WSSV-tolerant shrimp are still under development and are not commercially available (20). The domestic development and international import of specific pathogen-free (SPF) shrimp stocks has mitigated some disease outbreaks. However, even with routine rigorous screening disease continues to be a major threat. For instance, shrimp stocks in Brazil and Colombia were reported to be contaminated from imported SPF shrimp with underlying TSV infection that went undetected (21). The more recently documented spread of WSSV in Australia, India, and Ecuador has resulted in the virus being labeled as the most devasting pathogen in the aquacultural history of shrimp farming (22–24). To ensure globally distributed stocks are disease-free and to mitigate production losses for improved food security, it is crucial that rapid, accurate, and sensitive diagnostics are available to shrimp farmers (25, 26).

To address the need for rapid diagnostics in shrimp aquaculture, SHERLOCK technology has recently been applied to the detection of common and deadly shrimp viruses but remains to be optimized. For example, a CRISPR-based diagnostic was developed to detect *Vibrio* spp. that cause acute hepatopancreatic necrosis disease in shrimp but requires a two-step process of first amplifying pathogen DNA with recombinase polymerase amplification (RPA) and then detecting the amplicons with Cas12a in a separate reaction to detect down to 1000 copies per reaction (20 copies per μL in a 50 μL reaction) in 2 h (27). Our lab developed a different variation of a CRISPR-based diagnostic to detect WSSV in shrimp tissue that uses RPA to amplify WSSV DNA, RNA polymerase to transcribe amplicons to RNA, and Cas13a to detect transcribed amplicons (SHERLOCKv1) all in one tube (one-pot format) (28). This one-pot format reduces time-to-result and was able to detect 10 viral copies per reaction in 60 min. Other reports have found LAMP to be superior to RPA in speed and sensitivity (29, 30), and a second-generation SHERLOCK assay that couples LAMP with a heat tolerant Cas enzyme, Cas12b, showed highly sensitive, rapid, and robust detection of viral RNA from SARS-CoV-2 (31). Building upon these successes, and incorporating second-generation SHERLOCK technology, we demonstrate the adaptability of this technology for both DNA and RNA viral targets and present 2 second-generation SHERLOCK (SHERLOCKv2) assays that detect WSSV and TSV. These robust, sensitive, and specific lab-based fluorescent assays can detect viral target in shrimp tissue in 30 min without the need for thermocycling. They also enable field-deployable conversion for improved diagnostic capabilities of viral outbreaks in aquaculture settings. This demonstration of assay adaptation for diverse shrimp diseases paves the way
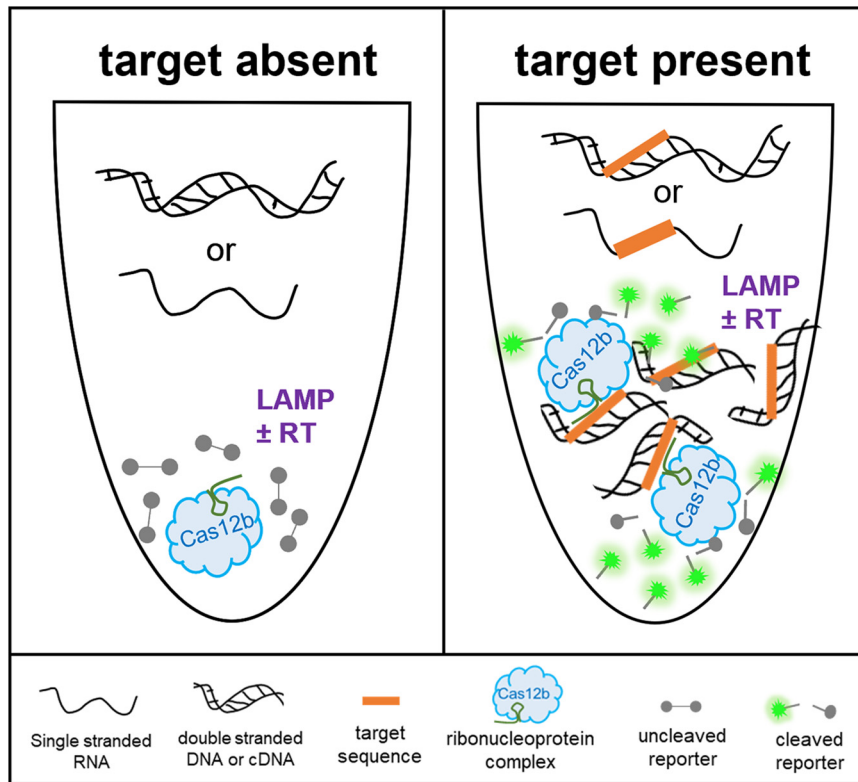
FIG 1 Schematic for CRISPR-based DNA and RNA detection in a one-pot reaction. When the TSV or WSSV target sequence is absent, there is no amplification and no CRISPR-Cas mediated cleavage of the reporter molecule. When the TSV or WSSV target sequence is present, there is isothermal amplification of the target sequence and simultaneous detection by CRISPR-Cas target binding and collateral cleavage of a fluorescent reporter. LAMP ± RT signifies the need for reverse transcriptase (RT) and LAMP for the amplification of the TSV RNA target or need for LAMP only for the amplification of the WSSV DNA target.

for next generation assay development in veterinary pathology and animal diagnostics for improved disease management in aquaculture and agriculture.

RESULTS

Diagnostic assay development. Combining the robustness of LAMP with the specificity of CRISPR and detection of Cas12b collateral cleavage activity, we developed sensitive and specific one-pot SHERLOCKv2 assays for the detection of DNA and RNA viruses that negatively impact shrimp aquaculture worldwide, WSSV and TSV (Fig. 1). In an initial screen to identify an optimal LAMP primer set targeting a conserved TSV genome region, we compared the amplification activity of three primer sets as well as a previously published LAMP primer set (32). We found the previously published set targeting the capsid protein gene between VP1 and VP3 domains showed the fastest, most sensitive detection of TSV and selected this set for the SHERLOCKv2 assay (Fig. 2a and c). In designing the WSSV assay, the highly conserved viral protein 28 (VP28) was targeted to limit the ability of WSSV strain to influence detection. Of the four LAMP primer sets designed and screened, one set (VP28.31) showed superior speed (Fig. 2b and d). The addition of poly-T linkers between the two annealing sites within the FIP and BIP primers increased both the speed and sensitivity of the primer set down to 100 copies (Fig. S1). Of the 12 guide RNAs designed to target within the TSV LAMP target region (Fig. S2a), one guide RNA (cr9225) produced cleavage signals before 30 min with low variance among replicate reactions and minimal background signal and was selected for the TSV SHERLOCKv2 assay (Fig. 3a). Of the 11 guide RNAs designed to target within the WSSV LAMP target region (Fig. S2b), one guide RNA (VP28_27) showed the highest cleavage signal with the greatest signal-to-background ratio and was
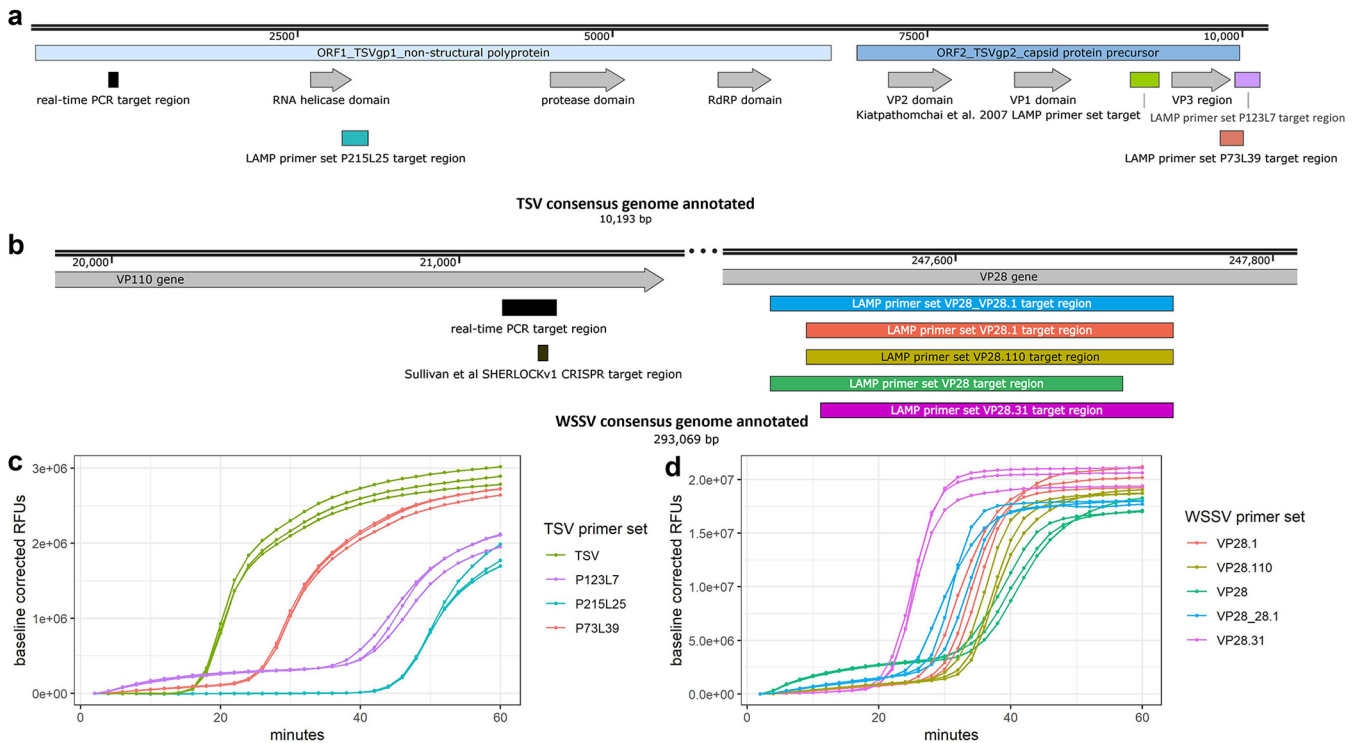
FIG 2 TSV and WSSV LAMP primer design and screening. (a) Annotated TSV consensus genome showing OIE standard diagnostic real-time PCR target region in black and LAMP target regions in teal, green, purple, and coral. (b) Annotated portions of WSSV consensus genome showing OIE standard diagnostic real-time PCR target region in black, the SHERLOCKv1 target region in brown, and LAMP target regions in blue, coral, gold, green, and magenta. (c) Amplification plot of triplicate LAMP reactions screening four different TSV primer sets (indicated by different colors) using 1,000,000 target copies of TSV. (d) Amplification plot of triplicate LAMP reactions screening five different WSSV primer sets (indicated by different colors) using 1,000,000 target copies of WSSV.

selected for the WSSV SHERLOCKv2 assay (Fig. 3b). Furthermore, we found that the addition of glycine, a reaction temperature of 62°C, 2 μM reporter concentration, and a guide RNA-to-Cas12b ratio of 1:1 consistently gave optimal signal-to-background in the WSSV SHERLOCKv2 assay. Because the addition of carrier nucleic acid has shown improvements to sensitivity and specificity in RT-LAMP reactions (33), we tested this in the TSV SHERLOCKv2 assay and found that the addition of 5 or 10 ng of nontarget carrier RNA produced the highest signal with the least variance among replicates (Fig. S3). For WSSV SHERLOCKv2 assay, we decided to use 20 ng of nontarget carrier DNA because that was the upper limit of input material reported in the WSSV SHERLOCKv1 limit-of-detection experiment and this amount would allow input for subsequent experiments to be standardized. A step-by-step protocol for SHERLOCK assay development is provided in the supplemental materials along with a table of all oligos and DNA sequences used (Table S1) and a table detailing all reaction components (Table S2).

Assay sensitivity and specificity. To evaluate assay sensitivity, we analyzed standard curves generated from 10-fold dilutions of the synthetic TSV target RNA (eight independent experiments) and synthetic WSSV target DNA (six independent experiments), and both assays consistently detected down to 100 copies for WSSV (200 copies for TSV) with a strong correlation to the amount of nucleic acid input (Fig. 4a and b; Fig. S4). We found synthetic target to be comparable to genomic target isolated from shrimp with high TSV and WSSV viral loads previously quantified by qPCR, confirming that synthetic target can be used for estimating TSV and WSSV copy number quantity in genomic samples (Fig. S4). In experiments evaluating assay specificity, both SHERLOCKv2 assays showed high specificity for their target pathogen. Only TSV-infected and WSSV-infected shrimp samples showed Cas12b collateral cleavage signal compared to samples from shrimp infected with other common shrimp pathogens (IMNV, IHHNV, EHP, and *Vibrio parahaemolyticus* causing AHPND/EMS) (Fig. 4c and d). Furthermore, both assays showed
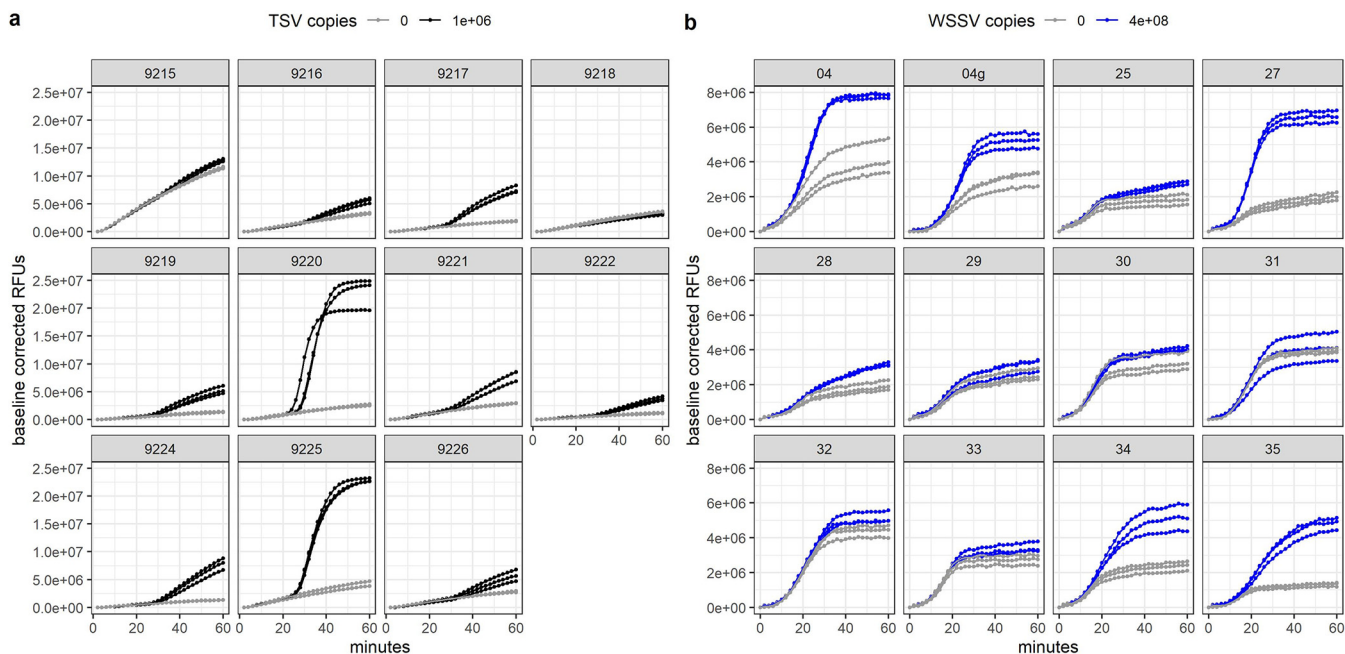
FIG 3 TSV and WSSV guide RNA screening. (a) Plots showing Cas12b collateral cleavage activity of each different TSV guide RNA when 1,000,000 (black) or 0 (gray) copies of TSV RNA target is present. (b) Plots showing Cas12b collateral cleavage activity of each different WSSV guide RNA when 400,000,000 (blue) or 0 (gray) copies of WSSV DNA target is present. "04g" is the same sequence as "04" but it was transcribed from a gBlock instead of an amplicon (see *Materials and Methods* for more details).

no false-positive detection in samples from specific pathogen-free shrimp (Fig. 4c and d). While we did observe stochastic nonspecific LAMP signal in some true negative samples, this did not lead to Cas cleavage and did not result in positive viral detection (Fig. S5).

Assay validation. To estimate the diagnostic sensitivity of the SHERLOCKv2 assays, we tested shrimp samples from different TSV and WSSV challenge experiments in SHERLOCKv2 assays and in the OIE (World Organization for Animal Health) recommended real-time PCR diagnostic for TSV and WSSV (34). Assays were run alongside standard curves to quantify and compare viral copy number determined by each method (real-time PCR hereinafter referred to as qPCR). With regard to the TSV challenge experiments, there are lines of shrimp that show a continuum of susceptibility and resistance depending on the line's genetics and the TSV strain used to evaluate susceptibility (35). We therefore used two different genetic lines with two different isolates that represent two extremes of disease continuum. The Belize isolate used to infect the TSV-tolerant *P. vannamei* line is known to be highly virulent and has led to TSV infection in TSV-tolerant commercial *P. vannamei* lines, where the TSV-susceptible Kona line has shown high rates of infection regardless of the TSV isolate used in challenge experiments (36). Following viral challenge, the TSV-susceptible line displayed clinical manifestation of disease, including pathognomonic lesions of TSV characterized by necrosis, pyknosis, and karyorrhexis of the cuticular epithelium within the appendages, gills, and exocuticle (Fig. 5a). In addition, some of these showed mortalities during the course of the experiment. However, the TSV-tolerant *P. vannamei* showed no TSV-associated pathognomonic lesions or mortalities (Fig. 5b). Because of the wide dynamic range in viral load expected in these samples, we did a titration experiment to determine an optimal amount of sample input for TSV detection with the TSV SHERLOCK assay. We determined that 10 ng of TSV-infected shrimp genomic RNA led to the least variable and highest signal (Fig. S3), and this amount was used for subsequent TSV SHERLOCKv2 and qPCR experiments. The qPCR detected TSV in all TSV-challenged shrimp samples (Fig. 5c; Table S3). The TSV SHERLOCK assay detected TSV in 26 out of the 30 TSV-challenged shrimp samples (87% positive percent agreement) (Table S3). The four samples for which SHERLOCK did not detect TSV had low viral load extrapolated from a qPCR standard curve (three had < 1,000 copies/μL and one had ~5,000 copies/μL). Both qPCR or SHERLOCK
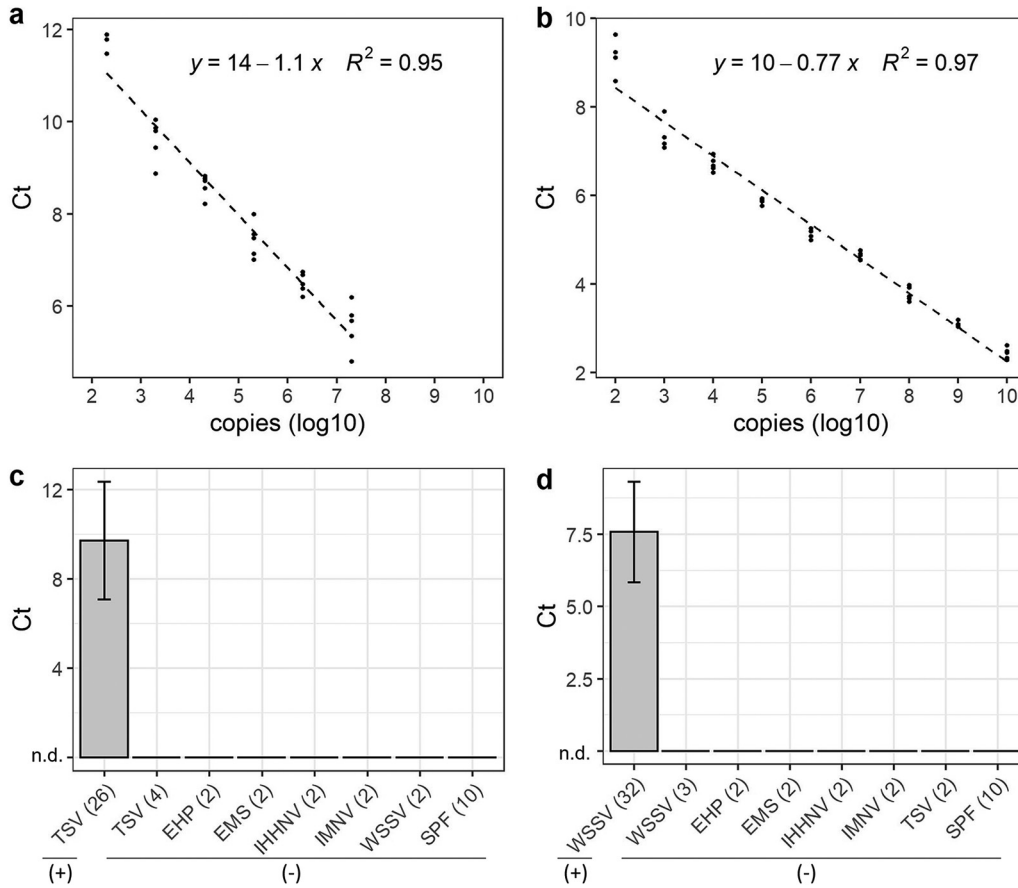
FIG 4 Sensitivity and specificity of SHERLOCK assays. SHERLOCK assay 10-fold standard curve showing Ct values for synthetic (a) TSV RNA and (b) WSSV DNA target with the dashed line indicating linear regression. Ct values (mean $+/-$ s.d.); n.d., not detected from SHERLOCK specificity tests evaluating the detection of (c) TSV and (d) WSSV in shrimp samples known to be infected with TSV, WSSV, and other common white shrimp pathogens, including *Vibrio* spp. (causing EMS), EHP, IHHNV, IMNV, and pathogen-free shrimp (SPF). (+) and (-) indicate SHERLOCK results.

TSV assays showed a significant effect of challenge experiment on the viral load (Mann-Whitney-U test $P = 0.006395$ and $P = 0.003415$, respectively), with the susceptible shrimp (Kona line) injected with the TSV El Salvador isolate generally showing a higher titer than the tolerant shrimp injected with the TSV Belize isolate. A Pearson's correlation analysis followed by a *t* test showed a statistically significant correlation between viral copy concentration predicted by SHERLOCK that predicted by qPCR ($R = 0.93$, $P = 1.5 \times 10^{-11}$; Fig. 5d) with SHERLOCK tending to underestimate viral copies relative to qPCR (Fig. 6a).

For WSSV, we tested the same WSSV-infected *P. vannamei* samples previously quantified by the OIE-recommended WSSV qPCR and the SHERLOCKv1 assay (28). Given that these samples previously showed high viral loads and sample material was limited, 1 ng of WSSV-infected shrimp genomic DNA was used in each SHERLOCKv2 reaction. Of the 35 WSSV-infected *P. vannamei* samples tested alongside standard curves, we detected infection in 32 samples (91% positive percent agreement) (Table S3). The three samples where no WSSV was detected were expected to have low viral copies based on qPCR estimations (~40, 50, and 800 copies/μL). Moreover, viral copy concentrations measured by WSSV SHERLOCKv2 were mostly similar to those quantified by qPCR (Fig. 6a). Compared to the previous version WSSV SHERLOCKv1 assay that used RPA and Cas13a enzymes (28), SHERLOCKv2 showed less variation across technical replicates than SHERLOCKv1 (Fig. 6b). A Pearson's correlation analysis followed by a *t* test showed a statistically significant correlation between SHERLOCKv2 and qPCR viral copy quantifications ($R = 0.79$, $P = 9.8 \times 10^{-8}$), and between SHERLOCKv2 and SHERLOCKv1 viral copy quantifications ($R = 0.75$, $P = 9.6 \times 10^{-7}$) (Fig. 7).
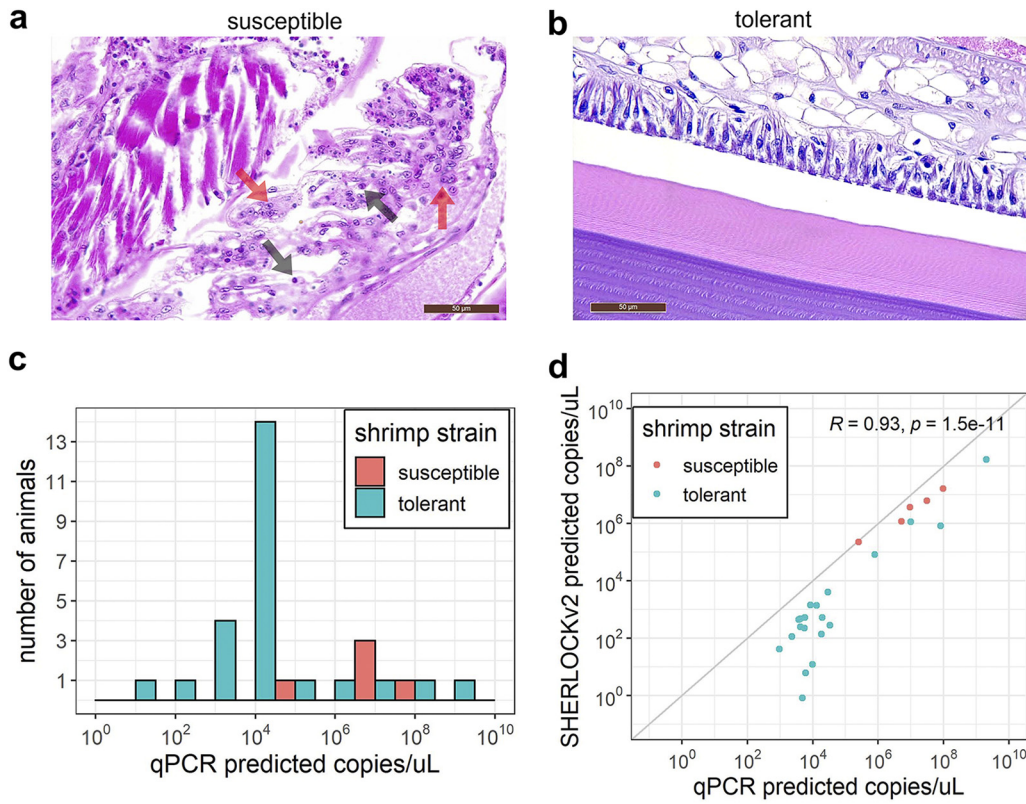
FIG 5 TSV SHERLOCK validation. (a) H & E-stained representative section from *P. vannamei* susceptible line after TSV exposure showing focal acute-phase infection in the gill characterized by spherical intracytoplasmic inclusions bodies (black arrows), pyknosis (red arrows) and karyorrhexis. (b) H & E-stained representative section from *P. vannamei* resistant line after TSV exposure showing no pathological signs characteristic of TSV infection. (c) TSV load quantified by qPCR in resistant (coral) and susceptible animals (teal). (d) Correlation between qPCR and TSV SHERLOCK quantification. Gray diagonal line indicates a 1:1 correlation.

DISCUSSION

With the goal of adapting cutting-edge human diagnostic technology to diseases impacting food security, we developed two different rapid and highly specific lab-based one-pot SHERLOCK fluorescent assays for the detection of common shrimp pathogens. We demonstrate the adaptability of the SHERLOCK platform for targeting
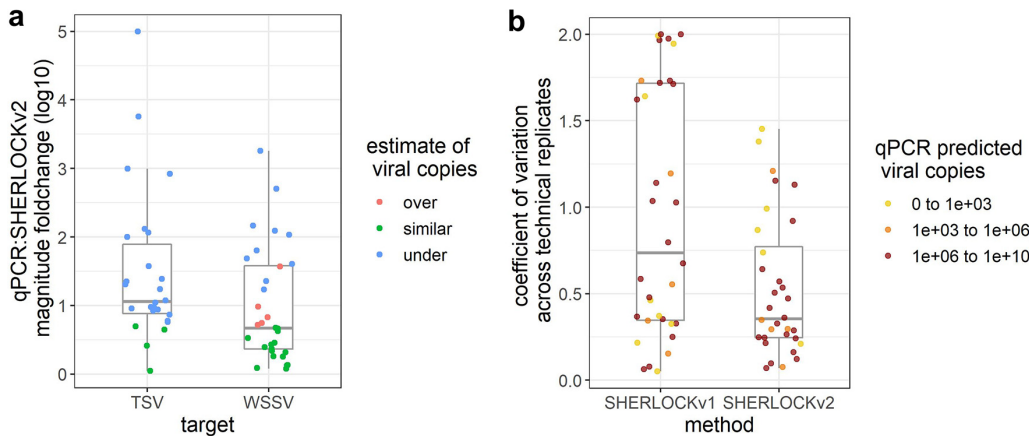

FIG 6 Comparison of SHERLOCKv2 assays to existing molecular assays. (a) Magnitude fold change in viral copies estimated by SHERLOCKv2 assays relative to qPCR assays for samples tested in both qPCR and SHERLOCK methods. (b) Variation across technical replicates for WSSV samples tested in both SHERLOCKv1 and SHERLOCKv2 assays.
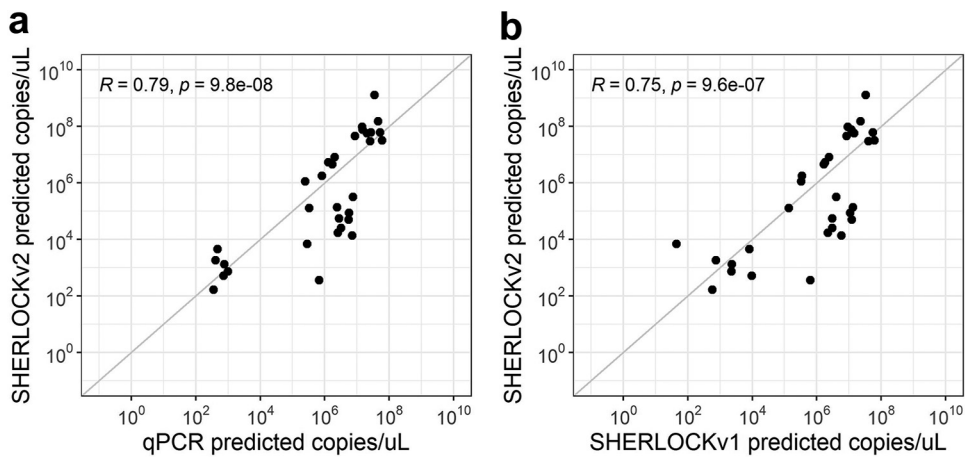
FIG 7 WSSV SHERLOCK assay validation. (a) Correlation between qPCR and WSSV SHERLOCKv2 assay quantification. (b) Correlation between WSSV SHERLOCKv2 and WSSV SHERLOCKv1 assays. Gray diagonal lines indicate a 1:1 correlation.

either a common RNA virus (TSV) or a common DNA virus (WSSV) that have impacted shrimp aquaculture globally. We found the TSV and WSSV SHERLOCKv2 assays to have a quantitative capability on par with the OIE-recommended qPCR assays for these diseases, albeit at seemingly less sensitivity which may be improved through further optimization. Moreover, both assays can assess infection status for a variety of samples in as little as 30 min, improving upon the time-to-result of qPCR. Without the need for thermocycling and with the demonstrated ease of converting a one-pot fluorescent SHERLOCK assay to a field-deployable assay (8, 28), these assays lay the foundation for rapid, specific field diagnostics in shrimp aquaculture.

Building on an earlier iteration of a WSSV SHERLOCK assay, we were able to simplify assay components leading to more robust and repeatable detection of both DNA and RNA viral targets. The previous WSSV SHERLOCK assay used RPA to amplify DNA target, RNA polymerase to convert the amplified target from DNA to RNA, and Cas13a to detect RNA target (28). The SHERLOCKv2 assays presented in this study use LAMP (with or without reverse transcriptase) and Cas12b to detect DNA target from RNA or DNA input, following the successful SARS-CoV-2 SHERLOCK assay design (31). By eliminating the need for converting input material to RNA and relying on Cas13a for RNA detection, these SHERLOCKv2 assays enable more stable and robust target detection. This is supported by the reduced variation across technical replicates observed for WSSV SHERLOCKv2 compared to WSSV SHERLOCKv1. Moreover, the use of LAMP in our assays makes them well-poised for use with a variety of sample types, including crude sample preparations. Although we did not test crude sample lysates in this study, we have previously successfully demonstrated a paper matrix DNA extraction method to be compatible with WSSV SHERLOCKv1. Given our past success and that the LAMP enzyme (Bst 2.0 polymerase) is highly tolerant to inhibitors (37, 38), we foresee these SHERLOCKv2 assays to be compatible with various sample types.

Pairing LAMP with CRISPR/Cas12b enabled these assays to overcome nonspecific signal that can occur in assays using LAMP alone. In the SHERLOCKv2 assays, stochastic nonspecific LAMP products did not lead to Cas cleavage signal. Although isothermal amplification-based methods recently developed for aquaculture diagnostics have shown that sequence-specific probes can enhance assay specificity (39, 40), the combination of primers and probes cannot always be relied on for sequence-specific detection (41). Cas detection systems rely on sequence-specific target binding to induce conformational change that triggers cleavage activity (42), and combining isothermal amplification methods with this additional layer of specificity is becoming more common in aquaculture molecular diagnostic approaches (28, 43). Despite reports of single insertion and deletion tolerance in some Cas complexes (44), we found Cas12b to be

highly specific, supportive of previous reports of Cas12b specificity down to the single nucleotide level (45).

Although disease diagnosis typically only requires a binary result, the ability to quantify viral load can be useful. The significant correlations we found between SHERLOCKv2 assays and qPCR assays suggest SHERLOCKv2 can be semiquantitative. The TSV SHERLOCKv2 assay tended to underestimate viral copies relative to qPCR while the WSSV SHERLOCKv2 assay mostly showed similar viral copies to qPCR. These discrepancies could be explained by differences in amplification efficiencies of different genomic target sequences. The TSV qPCR assay targets near the beginning of the ORF1 (TSVgp1) region whereas the TSV SHERLOCK assay targets near the end of the ORF2 region. The primers used for the OIE-recommended WSSV qPCR protocol were designed to target a genomic region ~20 kb upstream of the VP28 gene region, while the LAMP primers and guide RNA for the WSSV SHERLOCK assay target within the VP28 gene region itself. As amplification efficiency is affected by differences in structure and sequence length in target regions as well as primers, it can be expected that quantifications would differ between methods targeting different regions. Additionally, the structural differences in the synthetic target standards used in the SHERLOCK assays (200 to 300 DNA or RNA fragments) and qPCR assays (plasmids) could have contributed to discrepancies in results (46). Differences in data analysis between qPCR and SHERLOCKv2 methods could have also contributed to discrepancies in viral detection among the infected shrimp samples. Samples assessed in the qPCR assays were run in triplicate and considered to be positive if at least one replicate had a Ct value $\leq$ 40 for diagnosis (34), while samples assessed in the SHERLOCKv2 assays were run in quintuplicate and considered to be positive if at least three replicates passed a baseline and an outlier threshold. The intention of this SHERLOCK scoring criteria was to rigorously control for technical variation and precisely and confidently measure viral presence and abundance in the development of these new assays. If the criteria were relaxed to require only two samples passing the baseline threshold and not include an outlier threshold, TSV infection would have been found in 29/30 samples (97% positive percent agreement) and WSSV infection would have been found in 35/35 samples (100% positive percent agreement) (47). In the future, the SHERLOCK scoring criteria used here can likely be relaxed following the testing of larger number of samples. Similar to existing reports of the proportion of replicates testing positive being relative to target concentration in both SHERLOCK and qPCR assays (48, 49), the few samples with virus detected by qPCR and not by SHERLOCK were indeed closer to the LODs of both TSV and WSSV assays. Despite the differences in analysis methods and in the nature of template used to optimize the SHERLOCK assay compared to the qPCR assay, the binary qualitative results in detecting virus in shrimp tissue showed positive percent agreements (87% for TSV SHERLOCKv2 and 91% for WSSV SHERLOCKv2) and negative percent agreements (100% for both assays) within or close to the strict range required by the FDA for clinical SARS-CoV-2 assays (90% positive percent agreement and 95% negative percent agreement) (50). Moreover, the quantitative loads of the corresponding viruses as measured by the two assays were also comparable. This gives validity to the SHERLOCKv2 assays when compared to the current gold standard of TSV and WSSV detection recommended by the OIE.

With molecular diagnostics rapidly advancing alongside outbreaks of existing and emerging disease, the transfer of technology from human diagnostics to animal fields is critical, particularly to those that support global food security. With a growing need to support aquaculture production, we demonstrated the ability to adapt a SHERLOCK assay developed for human diagnostics for detecting RNA and DNA shrimp pathogens. This development of novel ($\pm$ RT)-LAMP + CRISPR/Cas diagnostic assays for TSV and WSSV monitoring in *P. vannamei* and potential for field-deployable conversion will accelerate biomonitoring for shrimp aquaculture and pave the way for the developing rapid, efficient diagnostics across the agriculture field.

MATERIALS AND METHODS

Viral challenge experiments. For TSV, two independent challenge experiments were conducted using *P. vannamei* lines that differ in TSV susceptibility and TSV isolates that differ in virulence. The

purpose of this was to generate tissues with a wide dynamic range of viral load. In one experiment, TSV-susceptible specific pathogen free (SPF) *P. vannamei* (Kona line) shrimp (N = 120) were injected with TSV inoculum (El Salvador isolate, Lightner et al. unpublished) intramuscularly and reared until animals were moribund (4 days). In a second experiment, individuals from a commercial line of TSV-tolerant SPF *P. vannamei* (N = 30) were injected with a TSV inoculum (Belize isolate [36]) intramuscularly. Shrimp were reared for 4 to 8 days in a single 1,600 L tank containing 1,000 L artificial seawater maintained at $27 \pm 1°C$ and a salinity of 30 ppt. No water change was done due to the short duration of the experiments. Shrimp tissues were processed for histopathology analysis following a standard procedure (51). Briefly, tissues were preserved in Davidson's AFA fixative for 48 h after which the fixative was replaced with an equal volume of 70% ethanol. Samples were then washed in a series of alcohol/xylene solutions, embedded in paraffin, and sectioned to 4 μm using a microtome. The tissue sections were stained with hematoxylin and eosin, and examined using a bright field light microscope. Histopathological evaluations were performed using a subset of samples from the experimentally infected tolerant *P. vannamei* (N = 6) and susceptible *P. vannamei* (N = 5). The severity of the TSV infection was graded based on a semiquantitative scale ranging from grade 0 to grade 4: grade 0 showing no signs of infection; grade 1 showing signs of infection by the pathogen but at levels that may be below those needed for clinical disease classification; grade 2 showing moderate signs of infection based on the number and severity of pathogen-caused lesions; grade 3 showing moderate to high signs of infection based on the number and severity of pathogen-caused lesions; and grade 4 showing high signs of infection based on a high number of pathogen-caused lesions and tissue destruction (52). Total RNA from experimentally TSV-challenged shrimp (N = 35) was extracted with the Total RNA purification kit (NORGEN BIOTEK CORP) following the manufacturer's recommendations. Quality and quantity were assessed using a NanoDrop (Thermo Fisher Scientific). The RNA concentrations of 30 samples were normalized to approximately 15 ng μL^{-1} and TSV was detected and quantified from 2 μL of sample using a TaqMan Fast Virus 1-Step Master Mix (Applied Biosystems) following the OIE recommended protocol and triplicate standards (mean $R^2 = 0.93 \pm 0.06$, mean efficiency 105.3% $\pm$ 15.28%) (53). All samples were run in triplicate alongside plasmid standards with known copy numbers (100 to 1,000,000 copies). TSV load in the experimentally challenged shrimp was calculated by extrapolating Ct values in the standard curve generated using plasmid DNA template.

Unlike TSV, all commercially available *P. vannamei* lines are highly susceptible to WSSV with shrimp mortality occurring 2 to 3 days postchallenge in routine bioassays conducted in the Aquaculture Pathology Laboratory at University of Arizona. Details of the viral challenge experiment with WSSV of *P. vannamei* are reported in Sullivan et al. (28). Briefly, specific pathogen free shrimp (N = 137) were challenged by feeding WSSV (China isolate CN95 [54]) infected tissue and reared under the same conditions and duration as described above. Infection was confirmed in moribund animals by histology as described above. Genomic DNA was extracted with the DNeasy blood and tissue kit (Qiagen), quantified using a NanoDrop (Thermo Fisher Scientific), and quantified by qPCR using 1 μL of sample with TaqMan Fast Virus 1-Step Master Mix run in triplicate on an ABI StepOne Plus system and following the OIE protocol using triplicate standards (mean $R^2 = 0.99 \pm 0.0007$, mean efficiency 90.6 $\pm$ 12.0%) (55).

TSV and WSSV SHERLOCK assay development. To identify genomic targets for TSV and WSSV viral detection, publicly available viral genome sequences were searched for consensus regions. For TSV, eight genomes were retrieved from GenBank (https://www.ncbi.nlm.nih.gov/genbank/; JF966384.1 [56], NC_003005.1 [57], JX094350.1 [58], AF277675.1 [57], GQ502201.1 [59], DQ104696.1 [60], AY997025.1 [61], DQ212790.1 [62]) and aligned with MAFFT (63) using the default parameters to generate a consensus sequence (Table S1). For WSSV, the highly conserved viral envelope protein 28 (64) was selected as a target and conservation across multiple strains was confirmed by surveying a consensus genome compiled from 10 different isolates as previously reported (28).

To generate candidate LAMP primer sets, target sequences were input into the NEB LAMP Primer Design tool (https://lamp.neb.com). For TSV, three LAMP primer sets were selected as well as a previously published LAMP primer set (32) for screening. For WSSV, four different candidate LAMP primer sets were selected and the primer set was optimized by testing sets containing different combinations of primers as well as primer modifications, including the addition of a poly-T linker between the F1c/B1c and F2/B2 annealing sites of the FIP and BIP primers (Table S1).

Guide RNAs for Cas12b collateral cleavage were designed using a sliding window of 20 bases in length and advancing one base at a time across the region between the F2 and B2 annealing sites of the LAMP FIP and BIP primers. To synthesize guide RNAs, a gBlock (IDT) containing the *Aap* Cas12b sgRNA scaffold sequence was first amplified using a forward primer containing the T7 promoter sequence and reverse primers containing each different spacer sequence. Amplification reaction conditions were as follows: 1× HF Buffer (NEB), 200 μM dNTPs (NEB), 0.5 μM forward primer, 0.5 μM reverse primer, 0.01 ng template DNA, and 1 unit Phusion DNA polymerase (NEB) in 50 μL. Reactions were run on a thermocycler (Applied Biosystems) with the following parameters: 98°C for 2 min, 30 cycles of 98°C for 10 s, 58°C for 30 s, and 72°C for 15 s, 72°C for 5 min, and a hold at 10°C. Products were gel purified using the QIAquick Gel Extraction kit (Qiagen) with a 2% agarose 1× TAE gel and products were eluted in 30 μL of Buffer EB pre-warmed to 50°C. Concentrations were measured using the Qubit Broad Range dsDNA kit (Life Technologies). Next, *in vitro* transcription reactions were performed using the Ampliscribe T7 flash transcription kit (Lucigen) in a 40 μL reaction with 50 ng of DNA template, 9 mM each ribonucleotide, 9 mM DTT, 1 μL of RiboGuard RNase inhibitor, 4 μL of T7 RNA polymerase, and 1× transcription reaction buffer. Reactions were run at 42°C for 4 h, incubated with 2 μL of DNase I (Lucigen) at 37°C for 15 min, and purified using the RNA Clean and Concentrate Kit (Zymo Research). Guide RNAs were quantified using the Qubit Broad Range RNA assay kit (Life Technologies) and molarity was estimated using the NEB copy

number converter (https://nebiocalculator.neb.com/). All sequences from the consensus genome, gBlocks (IDT), primers, and guide RNAs are listed in Table S1.

Evaluating LAMP primers. For TSV, primer sets were screened against a synthetic TSV RNA target *in vitro* transcribed from gBlock DNA (IDT, Table S1) using the Ampliscribe T7-Flash Transcription kit (Lucigen Corporation) and purified using the RNA Clean and Concentrator kit (Zymo Research) following manufacturer's instructions. For WSSV, primer sets were screened against either a synthetic WSSV DNA target (gBlock, IDT; Table S1) or genomic DNA isolated from shrimp with a high WSSV load. Target nucleic acid was diluted in background nucleic acid from SPF shrimp as detailed in Table S2e to improve the specificity of the LAMP primers. Total RNA from 10 SPF shrimp was isolated using the RNeasy blood and tissue kit (Qiagen) and genomic DNA from 10 SPF shrimp was isolated using the DNeasy blood and tissue kit (Qiagen). LAMP reactions were prepared as detailed in Table S2a and run at 60°C and 62°C (TSV and WSSV, respectively) for 1 h on a thermocycler for real-time PCR (QuantStudio 12K flex, Thermo Fisher Scientific) with fluorescent measurements taken at 2-min intervals. Successful primers were determined by their ability to start amplification before 30 min.

Evaluating guide RNAs and Cas12b detection. Guide RNAs were systematically evaluated with Recombinant *Aap* Cas12b (GenScript) for efficacy using TSV LAMP product or synthetic WSSV target DNA (gBlock, IDT) in 20 μL (TSV) or 10 μL (WSSV) reactions described Table S2b. Prior to adding template and reporter, reaction mixtures were incubated for 15 min at room temperature to facilitate the formation of the CRISPR/Cas ribonucleoprotein complex. For each guide RNA, a negative control was run that did not contain target nucleic acid to measure background collateral cleavage, and all reactions were run in triplicate. Reactions were run in a 384-well black clear bottom plate (Corning) at 60°C for 1 h with measurements recorded every 2 min using a Spectramax iD3 plate reader (Molecular Devices). Effective guide RNAs were identified as those that generate a signal well-distinguished from the negative control in less than 30 min.

Evaluating sensitivity and standard curve generation. To produce standard curves for each assay, one-pot LAMP-Cas12b SHERLOCK reactions were run using either *in vitro* transcribed synthetic TSV RNA target, synthetic WSSV DNA target (gBlock, IDT; Table S1), or genomic DNA isolated from shrimp with a high viral load. 10-fold dilution series of synthetic DNA or RNA were made ranging from 10^1 to 10^6 copies μL^{-1} (TSV) or 10^1 to 10^{10} copies μL^{-1} (WSSV) with all samples diluted in specific pathogen free shrimp genomic RNA (5 ng per 20 μL reaction for TSV) or DNA (20 ng per 20 μL reaction for WSSV). Negative-control reactions that did not contain any target nucleic acid were included in each experiment. Reactions were run with five replicates per sample prepared as detailed in Table S2c and run at 60°C (TSV) or 62°C (WSSV) using a QuantStudio 12k Flex thermocycler for real-time PCR (Applied Biosystems) for 60 min, with fluorescence readings every 2 min. Prior to adding dNTPs, *Bst* 2.0 DNA polymerase (New England BioLabs), primer mix, fluorescent reporter, SYTO-82 dye, or DNA, other reaction components were combined and incubated for 15 min at room temperature to facilitate the formation of the CRISPR/Cas ribonucleoprotein complex.

Evaluating SHERLOCK quantification. To compare quantification of viral loads estimated by the OIE-recommended qPCR and SHERLOCK, one-pot TSV SHERLOCK reactions were run on the same RNA samples from 30 TSV-infected shrimp quantified by qPCR described above. For WSSV, one-pot SHERLOCK reactions were run on the same DNA samples from 35 WSSV-infected shrimp previously quantified by qPCR (28). To standardize input across samples, 10 ng of RNA (TSV) or 1 ng of DNA (WSSV) was added per 20 μL SHERLOCK reaction. SHERLOCK reactions were prepared as detailed in Table S2c, and all samples were run alongside standard curves as described above. A linear regression analysis was performed on Ct values from the standard curve samples calculated from fluorescent measurements that were corrected to a baseline defined by cycles 1 to 2 for WSSV and 1 to 4 for TSV, and viral copies were estimated for each sample from the extrapolated standard Ct values. For each sample, including standards, any replicate outlier based on a Ct value beyond the sample median Ct $\pm$ one cycle was excluded and only samples with at least three out of five replicates were considered in downstream analyses. Viral copies estimated by SHERLOCK one-pot reactions were then compared to those estimated by qPCR using a Pearson correlation analysis followed by *t* test with the stat_cor function in the R package ggpubr (65).

Evaluating specificity. The specificity of each one-pot SHERLOCK assay was tested against either RNA or DNA extracted from shrimp tissue infected with infectious myonecrosis virus (IMNV; muscle tissue), infectious hypodermal and haematopoietic necrosis virus (IHHNV; muscle tissue), *V. parahaemolyticus* causing acute hepatopancreatic necrosis disease/early mortality syndrome (AHPND/EMS; hepatopancreas tissue), and *Enterocytozoon hepatopenaei* (EHP; hepatopancreas tissue). RNA was extracted using RNeasy mini plus kit (Qiagen) and DNA was extracted using the Qiagen DNeasy blood and tissue kit following manufacturer's protocols. One-pot reactions were prepared as detailed in Table S2c with a total of 10 ng of sample RNA (TSV) or 1 ng of sample DNA (WSSV) in each reaction. To estimate false-positive rates, one-pot reactions were prepared as detailed in Table S2c and run as described above with 5 ng of total RNA or 20 ng of genomic DNA isolated from muscle tissue from 10 individual specific pathogen-free shrimp.

Data availability. Raw fluorescence data from all qPCR and SHERLOCK experiments, intermediate files, R code used to generate plots and statistics, and all supplementary material including all sequences used in this study are publicly available at https://doi.org/10.5281/zenodo.7438263 (47).

SUPPLEMENTAL MATERIAL

Supplemental material is available online only.

SUPPLEMENTAL FILE 1, PDF file, 2.4 MB.

REFERENCES

1. Singh M, Bindal G, Misra CS, Rath D. 2022. The era of Cas12 and Cas13 CRISPR-based disease diagnosis. Crit Rev Microbiol 48:714–729. https://doi.org/10.1080/1040841X.2021.2025041.
2. Warke D. 2022. CRISPR-based tools: alternative methods for diagnosis of diseases. The Pharma Innovation J 11:1891–1896.
3. Cunha MV, Inácio J. 2015. Overview and challenges of molecular technologies in the veterinary microbiology laboratory. In Cunha M, Inácio J (eds), Veterinary infection biology: molecular diagnostics and high-throughput strategies. Methods in Molecular Biology, vol 1247. Humana Press, New York, NY. https://doi.org/10.1007/978-1-4939-2004-4_1.
4. Esbin MN, Whitney ON, Chong S, Maurer A, Darzacq X, Tjian R. 2020. Overcoming the bottleneck to widespread testing: a rapid review of nucleic acid testing approaches for COVID-19 detection. RNA 26:771–783. https://doi.org/10.1261/rna.076232.120.
5. Jayamohan H, Lambert CJ, Sant HJ, Jafek A, Patel D, Feng H, Beeman M, Mahmood T, Nze U, Gale BK. 2021. SARS-CoV-2 pandemic: a review of molecular diagnostic tools including sample collection and commercial response with associated advantages and limitations. Anal Bioanal Chem 413:49–71. https://doi.org/10.1007/s00216-020-02958-1.
6. Cammilleri G, Ferrantelli V, Pulvirenti A, Drago C, Stampone G, del Rocio Quintero Macias G, Drago S, Arcoleo G, Costa A, Geraci F, di Bella C. 2020. Validation of a commercial loop-mediated isothermal amplification (LAMP) assay for the rapid detection of Anisakis spp. DNA in processed fish products. Foods 9:92. https://doi.org/10.3390/foods9010092.
7. Gootenberg JS, Abudayyeh OO, Lee JW, Essletzbichler P, Dy AJ, Joung J, Verdine V, Donghia N, Daringer NM, Freije CA, Myhrvold C, Bhattacharyya RP, Livny J, Regev A, Koonin EV, Hung DT, Sabeti PC, Collins JJ, Zhang F. 2017. Nucleic acid detection with CRISPR-Cas13a/C2c2. Science 356:438–442. https://doi.org/10.1126/science.aam9321.
8. de Puig H, Lee RA, Najjar D, Tan X, Soenksen LR, Angenent-Mari NM, Donghia NM, Weckman NE, Ory A, Ng CF, Nguyen PQ, Mao AS, Ferrante TC, Lansberry G, Sallum H, Niemi J, Collins JJ. 2021. Minimally instrumented SHERLOCK (miSHERLOCK) for CRISPR-based point-of-care diagnosis of SARS-CoV-2 and emerging variants. Sci Adv 7. https://doi.org/10.1126/sciadv.abh2944.
9. FAO. 2020. The state of world fisheries and aquaculture 2020. Sustainability in action. www.fao.org.
10. Naylor RL, Kishore A, Sumaila UR, Issifu I, Hunter BP, Belton B, Bush SR, Cao L, Gelcich S, Gephart JA, Golden CD, Jonell M, Koehn JZ, Little DC, Thilsted SH, Tigchelaar M, Crona B. 2021. Blue food demand across geographic and temporal scales. Nat Commun 12:1–14. https://doi.org/10.1038/s41467-021-26063-8.
11. Stentiford GD, Neil DM, Peeler EJ, Shields JD, Small HJ, Flegel TW, Vlak JM, Jones B, Morado F, Moss S, Lotz J, Bartholomay L, Behringer DC, Hauton C, Lightner DV. 2012. Disease will limit future food supply from the global crustacean fishery and aquaculture sectors. J Invertebr Pathol 110:141–157. https://doi.org/10.1016/j.jip.2012.03.013.
12. NOAA Fisheries. 2022. Fisheries of the United States, 2020. US Department of Commerce, NOAA Current Fishery Statistics No. 2020.
13. Lafferty KD, Harvell CD, Conrad JM, Friedman CS, Kent ML, Kuris AM, Powell EN, Rondeau D, Saksida SM. 2015. Infectious diseases affect marine fisheries and aquaculture economics. Annu Rev Mar Sci 7:471–496. https://doi.org/10.1146/annurev-marine-010814-015646.
14. Hasson KW, Lightner DV, Mohney LL, Redman RM, Poulos BT, White BM. 1999. Taura syndrome virus (TSV) lesion development and the disease cycle in the Pacific white shrimp Penaeus vannamei. Dis Aquat Org 36:81–93. https://doi.org/10.3354/dao036081.
15. Zhan W-B, Wang Y-H, Fryer JL, Yu K-K, Fukuda H, Meng Q-X. 1998. White spot syndrome virus infection of cultured shrimp in China. J Aquat Anim Health 10:405–410. https://doi.org/10.1577/1548-8667(1998)010%3C0405:WSSVIO%3E2.0.CO;2.
16. Brock JA. 1997. Taura syndrome, a disease important to shrimp farms in the Americas. World J Microbiol Biotechnol 13:415–418. https://doi.org/10.1023/A:1018524216600.
17. Lightner DV, Redman RM, Pantoja CR, Tang KFJ, Noble BL, Schofield P, Mohney LL, Nunan LM, Navarro SA. 2012. Historic emergence, impact and current status of shrimp pathogens in the Americas. J Invertebr Pathol 110:174–183. https://doi.org/10.1016/j.jip.2012.03.006.
18. Tu C, Huang H-T, Chuang S-H, Hsu J-P, Kuo S-T, Li N-J, Hsu T-L, Li M-C, Lin S-Y. 1999. Taura syndrome in Pacific white shrimp Penaeus vannamei cultured in Taiwan. Dis Aquat Org 38:159–161. https://doi.org/10.3354/dao038159.
19. Argue BJ, Arce SM, Lotz JM, Moss SM. 2002. Selective breeding of Pacific white shrimp (Litopenaeus vannamei) for growth and resistance to Taura Syndrome Virus. Aquaculture 204:447–460. https://doi.org/10.1016/S0044-8486(01)00830-4.
20. Lillehammer M, Bangera R, Salazar M, Vela S, Erazo EC, Suarez A, Cock J, Rye M, Robinson NA. 2020. Genomic selection for white spot syndrome virus resistance in Whiteleg shrimp boosts survival under an experimental challenge test. Sci Rep 10. https://doi.org/10.1038/s41598-020-77580-3.
21. Eswaran S. 2021. Specific pathogen free (SPF) shrimps in aquaculture, p 465–470. In Pandey P, Parhi J (ed), Advances in fisheries biotechnology. Springer, Singapore.
22. Sivakumar S, Vimal S, Abdul Majeed S, Santhosh Kumar S, Taju G, Madan N, Rajkumar T, Thamizhvanan S, Shamsudheen K v, Scaria V, Sivasubbu S, Sahul Hameed AS. 2018. A new strain of white spot syndrome virus affecting Litopenaeus vannamei in Indian shrimp farms. J Fish Dis 41:1129–1146. https://doi.org/10.1111/jfd.12811.
23. Restrepo L, Reyes A, Bajaña L, Betancourt I, Bayot B. 2018. Draft genome sequence of a White Spot Syndrome Virus isolate obtained in Ecuador. Genome Announc 6. https://doi.org/10.1128/genomeA.00605-18.
24. Oakey HJ, Smith CS. 2018. Complete genome sequence of a white spot syndrome virus associated with a disease incursion in Australia. Aquaculture 484:152–159. https://doi.org/10.1016/j.aquaculture.2017.11.009.
25. Jacobson RH, Wright P. 2022. Principles and methods of validation of diagnostic assays for infectious diseases, p 11–26. In OIE Aquatic Animal Health Standards Commission (ed), Manual of diagnostic tests for aquatic animals. World Organization of Animal Health (Office International des Epizooties), Paris, France.
26. Flegel TW. 2019. A future vision for disease control in shrimp aquaculture. J World Aquacult Soc 50:249–266. https://doi.org/10.1111/jwas.12589.

27. Li C, Lin N, Feng Z, Lin M, Guan B, Chen K, Liang W, Wang Q, Li M, You Y, Chen Q. 2022. CRISPR/Cas12a based rapid molecular detection of acute hepatopancreatic necrosis disease in shrimp. Front Vet Sci 8:1693. https://doi.org/10.3389/fvets.2021.819681.

28. Sullivan TJ, Dhar AK, Cruz-Flores R, Bodnar AG. 2019. Rapid, CRISPR-based, field-deployable detection of white spot syndrome virus in shrimp. Sci Rep 9:1–7. https://doi.org/10.1038/s41598-019-56170-y.

29. Howson ELA, Kurosaki Y, Yasuda J, Takahashi M, Goto H, Gray AR, Mioulet V, King DP, Fowler VL. 2017. Defining the relative performance of isothermal assays that can be used for rapid and sensitive detection of foot-and-mouth disease virus. J Virol Methods 249:102–110. https://doi.org/10.1016/j.jviromet.2017.08.013.

30. Zou Y, Mason MG, Botella JR. 2020. Evaluation and improvement of isothermal amplification methods for point-of-need plant disease diagnostics. PLoS One 15:e0235216. https://doi.org/10.1371/journal.pone.0235216.

31. Joung J, Ladha A, Saito M, Kim N-G, Woolley AE, Segel M, Barretto RPJ, Ranu A, Macrae RK, Faure G, Ioannidi EI, Krajeski RN, Bruneau R, Huang M-LW, Yu XG, Li JZ, Walker BD, Hung DT, Greninger AL, Jerome KR, Gootenberg JS, Abudayyeh OO, Zhang F. 2020. Detection of SARS-CoV-2 with SHERLOCK one-pot testing. N Engl J Med 383:1492–1494. https://doi.org/10.1056/NEJMc2026172.

32. Kiatpathomchai W, Jareonram W, Jitrapakdee S, Flegel TW. 2007. Rapid and sensitive detection of Taura syndrome virus by reverse transcription loop-mediated isothermal amplification. J Virol Methods 146:125–128. https://doi.org/10.1016/j.jviromet.2007.06.007.

33. Wei S, Suryawanshi H, Djandji A, Kohl E, Morgan S, Hod EA, Whittier S, Roth K, Yeh R, Alejaldre JC, Fleck E, Ferrara S, Hercz D, Andrews D, Lee L, Hendershot KA, Goldstein J, Suh Y, Mansukhani M, Williams Z. 2021. Field-deployable, rapid diagnostic testing of saliva for SARS-CoV-2. Sci Rep 11:1–9. https://doi.org/10.1038/s41598-021-84792-8.

34. Tang-Nelson F-J, Lo C-F. 2021. Manual of diagnostic tests for aquatic animals 2021, 8th ed. World Organization of Animal Health (Office International des Epizooties), Geneva, Switzerland. Retrieved 22 June 2022.

35. Moss SM, Doyle RW, Lightner DV. 2005. Breeding shrimp for disease resistance: challenges and opportunities for improvement. Diseases in Asian Aquaculture V:379–393.

36. Srisuvan T, Noble BL, Schofield PJ, Lightner DV. 2006. Comparison of four Taura syndrome virus (TSV) isolates in oral challenge studies with Litopenaeus vannamei unselected or selected for resistance to TSV. Dis Aquat Organ 71:1–10. https://doi.org/10.3354/dao071001.

37. Kaneko H, Kawana T, Fukushima E, Suzutani T. 2007. Tolerance of loop-mediated isothermal amplification to a culture medium and biological substances. J Biochem Biophys Methods 70:499–501. https://doi.org/10.1016/j.jbbm.2006.08.008.

38. Tanner N. 2015. Improved reagents for Isothermal DNA amplification. New England Biolabs 1–3. https://www.neb-online.de/wp-content/uploads/2015/04/NEB_isothermal_amp.pdf.

39. Zhang T, Liu X, Yang X, Liu F, Yang H, Li X, Feng H, Wu X, Jiang G, Shen H, Dong J. 2022. Rapid on-site detection method for White Spot Syndrome Virus using Recombinase Polymerase Amplification combined with lateral flow test strip technology. Front Cell Infect Microbiol 12:1008. https://doi.org/10.3389/fcimb.2022.889775.

40. Kampeera J, Dangtip S, Suvannakad R, Khumwan P, Senapin S, Kiatpathomchai W. 2021. Reverse transcription loop-mediated isothermal amplification (RT-LAMP) combined with colorimetric gold nanoparticle (AuNP) probe assay for visual detection of tilapia lake virus (TiLV) in Nile and red hybrid tilapia. J Fish Dis 44. https://doi.org/10.1111/jfd.13482.

41. Hardinge P, Murray JAH. 2019. Lack of specificity associated with using molecular beacons in loop mediated amplification assays. BMC Biotechnol 19. https://doi.org/10.1186/s12896-019-0549-z.

42. Saha A, Arantes PR, Hsu RV, Narkhede YB, Jinek M, Palermo G. 2020. Molecular dynamics reveals a DNA-induced dynamic switch triggering activation of CRISPR-Cas12a. J Chem Inf Model 60:6427–6437. https://doi.org/10.1021/acs.jcim.0c00929.

43. Naranitus P, Aiamsa-At P, Sukonta T, Hannanta-Anan P, Chaijarasphong T. 2022. Smartphone-compatible, CRISPR-based platforms for sensitive detection of acute hepatopancreatic necrosis disease in shrimp. J Fish Dis 45:1805–1816. https://doi.org/10.1111/jfd.13702.

44. Zhang W, Shi R, Dong K, Hu H, Shu W, Mu Y, Yan B, Li L, Xiao X, Wang H. 2022. The off-target effect of CRISPR-Cas12a system toward insertions and deletions between target DNA and crRNA sequences. Anal Chem 94:8596–8604. https://doi.org/10.1021/acs.analchem.1c05499.

45. Teng F, Guo L, Cui T, Wang XG, Xu K, Gao Q, Zhou Q, Li W. 2019. CDetection: CRISPR-Cas12b-based DNA detection with sub-attomolar sensitivity and single-base specificity. Genome Biol 20:132. https://doi.org/10.1186/s13059-019-1742-z.

46. Bowers RM, Dhar AK. 2011. Effect of template on generating a standard curve for absolute quantification of an RNA virus by real-time reverse transcriptase-polymerase chain reaction. Mol Cell Probes 25:60–64. https://doi.org/10.1016/j.mcp.2010.12.002.

47. Trigg SA. 2022. shellytrigg/paper-TSV_WSSV_SHERLOCKv2: TSV-WSSV-SHERLOCKv2_ms (v5.0). Zenodo. https://doi.org/10.5281/zenodo.7438263.

48. Cowley JA, Rao M, Coman GJ. 2018. Real-time PCR tests to specifically detect IHHNV lineages and an IHHNV EVE integrated in the genome of Penaeus monodon. Dis Aquat Org 129:145–158. https://doi.org/10.3354/dao03243.

49. Lee RA, De Puig H, Nguyen PQ, Angenent-Mari NM, Donghia NM, McGee JP, Dvorin JD, Klapperich CM, Pollock NR, Collins JJ. 2020. Ultrasensitive CRISPR-based diagnostic for field-applicable detection of Plasmodium species in symptomatic and asymptomatic malaria. Proc Natl Acad Sci U S A 117.

50. Brooks ZC, Das S. 2020. COVID-19 testing impact of prevalence, sensitivity, and specificity on patient risk and cost. Am J Clin Pathol 154:575–584. https://doi.org/10.1093/ajcp/aqaa141.

51. Bell TA, Lightner DV. 1988. Handbook of normal penaeid shrimp histology. The World Aquaculture Society, Baton Rouge, LA.

52. Lightner DV. 1996. A handbook of shrimp pathology and diagnostic procedures for diseases of cultured penaeid shrimp. The World Aquaculture Society, Baton Rouge, LA.

53. Tang KFJ, Wang J, Lightner DV. 2004. Quantitation of Taura syndrome virus by real-time RT-PCR with a TaqMan assay. J Virol Methods 115:109–114. https://doi.org/10.1016/j.jviromet.2003.09.021.

54. Cruz-Flores R, Mai HN, Kanrar S, Aranguren Caro LF, Dhar AK. 2020. Genome reconstruction of white spot syndrome virus (WSSV) from archival Davidson's-fixed paraffin embedded shrimp (Penaeus vannamei) tissue. Sci Rep 10. https://doi.org/10.1038/s41598-020-70435-x.

55. Durand SV, Lightner DV. 2002. Quantitative real time PCR for the measurement of white spot syndrome virus in shrimp. J Fish Diseases 25:381–389. https://doi.org/10.1046/j.1365-2761.2002.00367.x.

56. Aranguren LF, Salazar M, Tang K, Caraballo X, Lightner D. 2013. Characterization of a new strain of Taura syndrome virus (TSV) from Colombian shrimp farms and the implication in the selection of TSV resistant lines. J Invertebr Pathol 112:68–73. https://doi.org/10.1016/j.jip.2012.08.009.

57. Mari J, Poulos BT, Lightner DV, Bonami JR. 2002. Shrimp Taura syndrome virus: genomic characterization and similarity with members of the genus Cricket paralysis-like viruses. J Gen Virol 83:915–926. https://doi.org/10.1099/0022-1317-83-4-915.

58. Tang KFJ, Navarro SA, Pantoja CR, Aranguren FL, Lightner DV. 2012. New genotypes of white spot syndrome virus (WSSV) and Taura syndrome virus (TSV) from the Kingdom of Saudi Arabia. Dis Aquat Organ 99:179–185. https://doi.org/10.3354/dao02470.

59. Dhar AK, Lakshman DK, Amundsen K, Robles-Sikisaka R, Kaizer KN, Roy S, Hasson KW, Allnutt FCT. 2010. Characterization of a Taura syndrome virus isolate originating from the 2004 Texas epizootic in cultured shrimp. Arch Virol 155:315–327. https://doi.org/10.1007/s00705-009-0584-5.

60. Huang XX, Lu CP. 2005. The molecular diagnosis and phylogenetic analysis of Taura Syndrome Virus isolated in China. https://www.ncbi.nlm.nih.gov/nuccore/DQ104696.1.

61. Srisuvan T, Tang KFJ, Lightner D. 2005. Experimental infection of Penaeus monodon with Taura syndrome virus (TSV). Dis Aquat Organ 67:1–8. https://doi.org/10.3354/dao067001.

62. Côté I, Navarro S, Tang KFJ, Noble B, Lightner DV. 2008. Taura syndrome virus from Venezuela is a new genetic variant. Aquaculture 284:62–67. https://doi.org/10.1016/j.aquaculture.2008.07.059.

63. Katoh K, Misawa K, Kuma KI, Miyata T. 2002. MAFFT: a novel method for rapid multiple sequence alignment based on fast Fourier transform. Nucleic Acids Res 30:3059–3066. https://doi.org/10.1093/nar/gkf436.

64. You Z, Nadala ECB, Yang J, Loh PC. 2004. Conservation of the DNA sequences encoding the major structural viral proteins of WSSV. Dis Aquat Organ 61:159–163. https://doi.org/10.3354/dao061159.

65. Alboukadel K. 2020. ggpubr: "ggplot2" Based Publication Ready Plots. R package version 0.4.0.